Surface Science 66 (1977) 253–271


# GENERALIZED LANGEVIN THEORY FOR GAS–SOLID PROCESSES: INELASTIC SCATTERING STUDIES

Barbara J. GARRISON and Steven A. ADELMAN *
*Department of Chemistry, Purdue University, West Lafayette, Indiana 47907, USA*

Received 28 January 1977

The generalized Langevin equations for describing gas solid processes are recast as coupled first order differential equations, which are soluble by standard classical trajectory techniques. Energy transfer in rare gas/metal collisions is studied for three computationally simple models: the heatbath Brownian oscillator (hBo) model which includes the effects of the lattice, the Einstein or uncoupled oscillator model and the friction model. The hBo model correctly gives the qualitative behavior of the energy transfer for all collision times; the Einstein model is correct for short collision times but not long ones; and the friction model is unreliable.

## 1. Introduction

Many-body dynamics must be realistically and simply included in any generally useful theoretical approach to gas–solid processes. The generalized Langevin theory developed elsewhere [1–4] provides a practical and flexible computational methodology for handling the many-body problem in gas–solid dynamics within the approximation of classical mechanics. Our purposes in this paper are to outline the main features of the Langevin method, to show clearly how a calculation may be performed, and to apply the technique to a numerical study of rare gas–metal collisions.

Our plan here is as follows: In section 2.1 we review the basic ideas underlying the generalized Langevin method. In section 2.2 we show how the terms appearing in the Langevin equation may be computed from the mode density of the solid. Section 2.3 and the Appendix deal with methods for reducing the Langevin equation to an effective few-body classical trajectory problem which may be solved by standard techniques. The key idea is that most of the solid may be modeled by one or a few optimally chosen Brownian oscillators. Section 2.4 is concerned with explicit evaluation of the quantities occurring in our theory for the Debye mode density. In section 2.5 we describe three simple solid models which emerge as natural approximations to the full generalized Langevin dynamics. Collisional

* Alfred P. Sloan Foundation Fellow.

results predicted by these models are compared in section 3 as part of our numerical study of rare gas–metal scattering. Finally, in section 4 we summarize our conclusions.

## 2. Generalized Langevin formalism

### 2.1. Langevin transformation

Underlying the Langevin approach is the fact that only a few (~1–6) of the many (~$10^{23}$) solid atoms are directly struck by the incident gas particle in a gas–solid collision. The struck or primary oscillators are, however, coupled to the remainder of the lattice which functions as a heatbath. The many-body problem in gas–solid dynamics, of course, arises from the many-body character of the heatbath.

Our basic idea is that the detailed motion of the heatbath need not be explicitly followed since only the *influence* of this motion on the collision is observable. This influence depends on only rather gross features of the heatbath's complex dynamics and thus may be simply modeled. Thus we solve the many-body problem by simulating the heatbath's influence rather than following its irrelevant motion.

To implement these ideas we transform the original many-body Newton equations of motion to an effective few-body form [1–4]. These new equations of motion involve only the dynamics of the gas particle and the struck oscillators explicitly. They contain, however, the heatbath influence and thus properly include the many-body effect. The advantage of the transformed dynamical equations is that they involve only a few degrees of freedom and may be solved using numerical methods familiar from conventional classical trajectory calculations [5], section 2.3.

The transformation to effective equations of motion may be carried through *exactly* for harmonic solids to yield (here we assume, for simplicity, a *single* struck oscillator in the primary zone)

$$m\ddot{\boldsymbol{r}}(t) = -m\omega_0^2 \boldsymbol{r}(t) - \nabla_r W(\boldsymbol{r}, \boldsymbol{R}) + m \int_0^t \boldsymbol{\Theta}(t-\tau)\cdot \boldsymbol{r}(\tau)\,\mathrm{d}\tau + \boldsymbol{f}(t), \tag{2.1a}$$

$$M\ddot{\boldsymbol{R}}(t) = -\nabla_R W(\boldsymbol{r}, \boldsymbol{R}), \tag{2.1b}$$

where $\boldsymbol{r} = (x,y,z)$ and $\boldsymbol{R} = (X,Y,Z)$ are the positions of the struck solid atom and the gas atom respectively, $m$ and $M$ are their respective masses and $\omega_0$ is the root mean square normal mode frequency of the solid. The coordinate system is oriented so that the $z$ (or $Z$) axis is perpendicular to the surface and the $x$ and $y$ ($X$ and $Y$) axes are in the plane of the surface. The potential $W(\boldsymbol{r},\boldsymbol{R})$ describes the interaction between the gas and solid. While it depends on the *instantaneous* positions of only the gas and primary lattice atoms, it may depend on the *equilibrium* positions of many solid atoms.

If the last two terms in eq. (2.1a) are dropped, the resulting equation describes scattering off one atom in an Einstein (uncoupled oscillator) solid with characteristic frequency $\omega_0$. The final two terms in eq. (2.1a) thus account for the influence of the heatbath.

The qualitative nature of the heatbath terms in eq. (2.1a) can be best understood if the solid is assumed to be at a temperature $T_s = 0$ K. The random force or noise term $f(t)$ is proportional to $\sqrt{T_s}$ so at $T_s = 0$ K it vanishes. If the atom in the primary zone is displaced its energy will randomize and eventually dissipate throughout the solid. This dissipation is accounted for by the damping kernel $\boldsymbol{\Theta}(t)$. As the solid temperature $T_s$ is increased this dissipation continues; however, at finite solid temperature the random force $f(t)$ allows energy flow from the heatbath to the primary atom. The dissipative and random forces are balanced so as to maintain the thermal equilibrium of the primary oscillators. The quantitative expression of this balance is the second fluctuation-dissipation theorem [3]

$$\langle f(t) f(0) \rangle = m k_B T_s \int_t^\infty \boldsymbol{\Theta}(\tau)\, d\tau, \tag{2.2}$$

where $\langle\ \rangle$ denotes a thermal average over heatbath initial conditions.

### 2.2. Connection with mode density

We next relate $\omega_0$, $\boldsymbol{\Theta}(t)$, and $f(t)$, the basic quantities appearing in the GLE (2.1), to the mode density $\rho(\omega)$ of the full solid. The relationships are particularly simple for isotropic solids and we restrict ourselves here to this case. The primitive frequency $\omega_0$ is simply the root mean square frequency

$$\omega_0 = \left( \int_0^\infty \omega^2 \rho(\omega)\, d\omega \right)^{1/2}. \tag{2.3}$$

The relationship between $\Theta(t)$ and $\rho(\omega)$ is conveniently established by introducing a spectral density $\sigma(\omega)$ characterizing the heatbath. This is defined by

$$\Theta(t) = \int_0^\infty \omega^{-1} \sigma(\omega) \sin \omega t\, d\omega. \tag{2.4}$$

We analogously define the susceptibility $\chi(t)$ of the primary atoms as

$$\chi(t) = \int_0^\infty \omega^{-1} \rho(\omega) \sin \omega t\, d\omega. \tag{2.5}$$

Here we have assumed that the solid is isotropic so that the tensors $\boldsymbol{\chi}(t) = \chi(t)\mathbf{1}$ and $\boldsymbol{\Theta}(t) = \Theta(t)\mathbf{1}$ are diagonal with all the diagonal elements equal. The following results

could also be derived for a general tensorial $\boldsymbol{\chi}(t)$ (or $\boldsymbol{\Theta}(t)$). As derived elsewhere [3] $\chi(t)$ and $\Theta(t)$ are related through their Laplace transforms, $\hat{\chi}(z)$ and $\hat{\Theta}(z)$ respectively, viz.,

$$\hat{\Theta}(z) = z^2 + \omega_0^2 - \hat{\chi}^{-1}(z). \tag{2.6}$$

Using eqs. (2.4)–(2.6) one obtains the relationship [6]

$$\sigma(\omega) = \rho(\omega)/|\hat{\chi}(i\omega)|^2. \tag{2.7}$$

Thus by knowing a mode density $\rho(\omega)$ for the entire solid one can obtain $\sigma(\omega)$ (eqs. (2.7) and (2.5)) and then obtain $\Theta(t)$ from eq. (2.4).

The noise source $f(t)$ is also generated from $\sigma(\omega)$. The noise is written as a Fourier transform [6]

$$f(t) = \pi^{-1} \int_0^{\omega_{\max}} d\omega |\tilde{f}(\omega)| \cos[\omega t - \delta(\omega)], \tag{2.8a}$$

where $\omega_{\max}$ is the maximum normal mode frequency of the solid. Evaluating the integral in eq. (2.8a) by Legendre–Gauss quadrature gives

$$f(t) = \pi^{-1} \omega_{\max} \sum_{\lambda=1}^{Q} W_\lambda |\tilde{f}(\omega_\lambda)| \cos[\omega_\lambda t - \delta(\omega_\lambda)], \tag{2.8b}$$

where $W_\lambda$ and $x_\lambda = \omega_\lambda/\omega_{\max}$ are the Legendre–Gauss weights and points respectively. The expansion (2.8b) allows convenient Monte Carlo sampling of $f(t)$. The phase shift $\delta(\omega_\lambda)$ is randomly picked from a uniform distribution with $0 \leqslant \delta(\omega_\lambda) \leqslant 2\pi$. The Fourier component $|\tilde{f}(\omega_\lambda)|$ is sampled from Gaussian distribution with variance $\Delta_\lambda$, where [6]

$$\Delta_\lambda = \left\{ \frac{2\pi^2 m k_B T}{W_\lambda} \left( \frac{\omega_{\max}}{\omega_\lambda} \right)^2 \omega_{\max}^{-3} \sigma(\omega_\lambda) \right\}^{1/2}. \tag{2.9}$$

By randomly picking $\delta(\omega_\lambda)$ (uniform distribution) and $|\tilde{f}(\omega_\lambda)|$ (Gaussian distribution) the initial conditions of the heatbath are sampled. The fluctuation-dissipation theorem (eq. (2.2)) is satisfied and thermal equilibrium maintained by determining both $\Theta(t)$ and $f(t)$ from the same spectral density, $\sigma(\omega)$.

One limitation of this scheme must be mentioned. The auto-correlation function $\langle f(t')f(t)\rangle$ computed from eq. (2.8b) will not satisfy the fluctuation-dissipation theorem for times $t - t' > \tau \cong Q\,\omega_D^{-1}$. We may avoid this pitfall by choosing $Q$ such that $\tau$ is much greater than a collision time; typically $Q = 48$. Generating an $f(t)$ from eq. (2.8b) with $Q = 48$ before each trajectory (see section 2.3) is inefficient. Several methods can be proposed to circumvent this problem. The random force $f(t)$ is an external force on the primary lattice and thus may be separately

computed and stored. In practice a few $f(t)$ strips valid for long times are generated at fixed time intervals and permanently stored. These strips are then randomly accessed and the appropriate number of time steps are stored in the computer for use during the trajectory calculation. If $Q$ were infinite, randomly accessing a single (infinite) $f(t)$ strip computed from a *particular* set of $\delta(\omega_\lambda)$ and $|\tilde{f}(\omega_\lambda)|$ would be equivalent to sampling all $\delta(\omega_\lambda)$ and $|\tilde{f}(\omega_\lambda)|$. This is not rigorously true for $Q$ finite; finite strips are biased by the initial conditions. This biasing can be minimized by sampling from several strips.

Alternately eq. (2.8b) can be expanded as

$$f(t) = \pi^{-1}\omega_{\max} \sum_{\lambda=1}^{Q} W_\lambda |\tilde{f}(\omega_\lambda)| \{\cos(\omega_\lambda t)\cos[\delta(\omega_\lambda)] + \sin(\omega_\lambda t)\sin[\delta(\omega_\lambda)]\} . \tag{2.8c}$$

The functions $\cos(\omega_\lambda t)$ and $\sin(\omega_\lambda t)$ are computed and stored at fixed time intervals. Before each trajectory $|\tilde{f}(\omega_\lambda)|$ and $\delta(\omega_\lambda)$ are sampled and a noise function $f(t)$ is computed from eq. (2.8c). This procedure eliminates the biasing problem inherent in the strip method described above. Moreover, it is quite efficient since the functions $\cos(\omega_\lambda t)$ and $\sin(\omega_\lambda t)$ need only be computed once. Both methods were employed in this study providing a useful numerical check.

Finally, in discussion of models (section 2.5) a friction constant $\beta$ and an effective frequency $\Omega$ are introduced. These are [3]

$$\beta = \lim_{z\to 0} \mathrm{d}\hat{\chi}^{-1}(z)/\mathrm{d}z , \tag{2.10a}$$

$$\Omega^2 = \lim_{z\to 0} \hat{\chi}^{-1}(z), \tag{2.10b}$$

and thus may be related to the mode density through eq. (2.5).

### 2.3. Method for dynamics

For ease in solving the GLE (2.1), the damping kernel $\Theta(t)$ computed from eq. (2.4) is fit to damped sine functions [6]; i.e.

$$\Theta(t) = \sum_{\lambda=1}^{N} C_\lambda \exp(-\gamma_\lambda t)\sin(\tilde{\omega}_\lambda t), \tag{2.11}$$

where $C_\lambda$, $\gamma_\lambda$, and $\tilde{\omega}_\lambda$ are determined by least squares fitting the expansion eq. (2.11) to a representation of $\Theta(t)$ obtained by numerically integrating eq. (2.4). The damped sine representation of $\Theta(t)$, eq. (2.11), has several advantages. First, (see below) it allows us to reduce the integral-differential Langevin equations (2.1) to a set of first order purely differential equations of the type familiar from conventional classical trajectory studies. These first order equations may be solved by standard numerical integration algorithms [7]. The physical reason for this simpli-

fication will become clear in our discussion of models in section 2.5 and the Appendix. Second, the damped sine expansion for $\Theta(t)$ decays to zero at long times; unphysical recurrences which occur for many approximate representations of lattice susceptibilities [6] do not arise. Third, the damped sine representation gives a good fit to $\Theta(t)$ for short times, even for $N = 1$. Since $\Theta(t)$ is small and oscillatory at long times, we believe that only its short time behavior importantly influences trajectory averaged collision dynamics. This is certainly true for the relatively short duration processes studied here. Finally, the fit to $\Theta(t)$, eq. (2.11), can be made increasingly accurate by including more terms in the sum.

Employing a finite truncation of eq. (2.11) for $\Theta(t)$ amounts to using a modified $\sigma(\omega)$ which is slightly different from that employed in the initial calculation of the exact $\Theta(t)$. Using the general relationship [6]

$$\sigma(\omega) = -2\pi^{-1}\,\omega\,\mathrm{Im}\,\hat{\Theta}(\mathrm{i}\omega)\,, \tag{2.12}$$

which follows from eq. (2.4), and using eq. (2.11) one finds that this modified spectral density $\sigma_f(\omega)$ is given by

$$\sigma_f(\omega) = 4\pi^{-1}\omega^2 \sum_{\lambda=1}^{N} \frac{C_\lambda \tilde{\omega}_\lambda \gamma_\lambda}{(\tilde{\omega}_\lambda^2 + \gamma_\lambda^2 - \omega^2)^2 + 4\gamma_\lambda^2\omega^2}\,. \tag{2.13}$$

To guarantee thermodynamic consistency, we employ $\sigma_f(\omega)$ in our sampling of $f(t)$; i.e., in eq. (2.9). Our approximation for $\Theta(t)$ also prescribes an approximate friction parameter $\beta_f$, eq. (2.10a), given by

$$\beta_f = 2\sum_{\lambda=1}^{N} \frac{C_\lambda \tilde{\omega}_\lambda \gamma_\lambda}{(\gamma_\lambda^2 + \tilde{\omega}_\lambda^2)^2}\,. \tag{2.14}$$

The short-time behavior of the primary lattice atom which is described by the frequency $\omega_0$ is independent of the particular approximate description of the heat-bath adopted. Hence, we may choose $\omega_0$ as before (from eq. (2.3)) using the *exact* $\rho(\omega)$, despite the fact that we are employing an approximate representation of $\sigma(\omega)$. We also employ the exact $\Omega$, eq. (2.10b), since the correct approximate $\Omega$ typically differs only slightly.

The functional form chosen for $\Theta(t)$, eq. (2.11) greatly simplifies the problem of solving the GLE. If $\Theta(t-\tau)$ may be written as a sum of functions separable to $t$ and $\tau$, then the GLE can be written as coupled first order differential equations soluble by standard classical trajectory techniques. A procedure based on this idea was presented by us elsewhere [6]. We adopt here, however, a related but different procedure due to Doll and Dion [8] which is computationally more efficient [9]. Using this method, the GLE may be recast as

$$\dot{\boldsymbol{p}}(t) = -m\omega_0^2 \boldsymbol{r}(t) - \nabla_r W(\boldsymbol{r}, \boldsymbol{R}) + m\sum_{\lambda=1}^{N} I_\lambda^s(t) + \boldsymbol{f}(t)\,, \tag{2.15a}$$

$$\dot{r}(t) = p(t)/m\,, \tag{2.15b}$$

$$\dot{P}(t) = -\nabla_R W(r, R)\,, \tag{2.15c}$$

$$\dot{R}(t) = P(t)/M\,, \tag{2.15d}$$

$$\dot{I}^s_\lambda(t) \equiv \frac{\mathrm{d}}{\mathrm{d}t}\{\int_0^t C_\lambda \exp[-\gamma_\lambda(t-\tau)]\sin[\tilde{\omega}_\lambda(t-\tau)]\, r(\tau)\,\mathrm{d}\tau\}$$

$$= -\gamma_\lambda I^s_\lambda(t) + \tilde{\omega}_\lambda I^c_\lambda(t)\,, \tag{2.15e}$$

$$\dot{I}^c_\lambda(t) \equiv \frac{\mathrm{d}}{\mathrm{d}t}\{\int_0^t C_\lambda \exp[-\gamma_\lambda(t-\tau)]\cos[\tilde{\omega}_\lambda(t-\tau)]\, r(\tau)\,\mathrm{d}\tau\}$$

$$= C_\lambda r(t) - \gamma_\lambda I^c_\lambda(t) - \tilde{\omega}_\lambda I^s_\lambda(t)\,, \tag{2.15f}$$

which are of the desired first order differential equation form.

### 2.4. Debye model

The above derivations are completely general and can be used if one has either $\rho(\omega)$ or $\sigma(\omega)$ [10]. For the calculations studied here, we use the bulk continuum or Debye model. Work is currently under way to include surface phonons within the continuum model. For the Debye model the normal mode spectrum is

$$\rho(\omega) = 3\omega_D^{-3}\omega^2\eta(\omega - \omega_D)\,, \tag{2.16}$$

where $\eta(x)$ is the unit step function, $\omega_D = k_B\Theta_D/\hbar$, and $\Theta_D$ is the Debye temperature. From eqs. (2.7) and (2.16)

$$\sigma(\omega) = 3\omega_D^{-3}\omega^2\eta(\omega - \omega_D)/|\hat{\chi}(\mathrm{i}\omega)|^2\,. \tag{2.17}$$

The Laplace transform of $\chi(t)$ for the Debye model may be derived from eqs. (2.5) and (2.16) to give [3]

$$\hat{\chi}(z) = 3\omega_D^{-3}[\omega_D - z\,\arctan(\omega_D/z)]\,. \tag{2.18}$$

Using eqs. (4.6.16) and (4.6.7), ref. [11], one obtains

$$|\hat{\chi}(\mathrm{i}\omega)|^2 = 9\omega_D^{-6}\{[\omega_D - \omega\,\mathrm{arccoth}(\omega^{-1}\omega_D)]^2 + (\tfrac{1}{2}\pi\omega)^2\}. \tag{2.19}$$

Eqs. (2.17) and (2.19) determine the Debye model $\sigma(\omega)$.

The damped sine representation for the Debye model $\Theta(t)$ is obtained by numerically integrating eq. (2.4) with $\sigma(\omega)$ from eqs. (2.17) and (2.19) and then fitting at short times the numerical $\Theta(t)$ to the expansion eq. (2.11). The one term fit used here is given in table 1.

The quantities $\omega_0$, eq. (2.3), and $\beta$, eq. (2.10a), may also be computed. Using eq.

Table 1
Parameters for $\Theta(t)$

| $N$ | $C_\lambda/\omega_D^3$ | $\gamma_\lambda/\omega_D$ | $\tilde{\omega}_\lambda/\omega_D$ |
|---|---|---|---|
| 1 | 0.16269 | 0.23599 | 0.59860 |

(2.16) one obtains for $\omega_0$

$$\omega_0 = \sqrt{(\tfrac{3}{5})}\omega_D. \tag{2.20}$$

The friction coefficient $\beta_D$ and effective frequency $\Omega_D$ for the Debye model are derived from eqs. (2.6), (2.10), and (2.18) as

$$\beta_0 = \tfrac{1}{6}\pi\omega_D, \tag{2.21a}$$

$$\Omega_D = \omega_D/\sqrt{3}. \tag{2.21b}$$

### *2.5 Solid models*

Three physical models for the solid may be derived as simple approximations to the full GLE formalism: the Einstein model, the friction model, and the heatbath Brownian oscillator model. For an Einstein solid the last two terms in (2.1a) (the many-body terms) are neglected. The only temperature effects come through the initial conditions of the oscillator (section 3). The Einstein model should be valid when the collision times are very short because the effect of the heatbath on the collision is not felt instantaneously. However, the Einstein model will break down with longer collision times.

For processes which are long on the timescale of a solid vibration, a local friction approximation [2,3] to the generalized Langevin dynamics *may* be reasonable. Within this approximation the gas–solid Langevin equations of motion (2.1) become [3]

$$m\ddot{\boldsymbol{r}}(t) = -m\Omega^2\boldsymbol{r}(t) - \nabla_r W(\boldsymbol{r}, \boldsymbol{R}) - m\beta\dot{\boldsymbol{r}}(t) + \boldsymbol{f}(t), \tag{2.22a}$$

$$M\ddot{\boldsymbol{R}}(t) = -\nabla_R W(\boldsymbol{r}, \boldsymbol{R}), \tag{2.22b}$$

where $\beta$ is found from eqs. (2.10a), (2.14) or (2.21a). This states that the struck solid atom instantaneously feels the effects of the heatbath. In contrast to the Einstein model, the friction model will fail for short collision times.

By expressing $\Theta(t)$ as an expansion in damped sine functions, eq. (2.11) and truncating the expansion at one term, a simple physical model emerges; the heatbath has the characteristics or response of a Brownian oscillator. This heatbath Brownian oscillator model is qualitatively correct for all times. Quantitatively, it is

valid for short times; the quantitative accuracy for long times requires further study. An important advantage of the heatbath Brownian oscillator model is great computational simplicity. Solving eqs. (2.15) with $N = 1$ is computationally equivalent to a three-particle classical trajectory problem. This reduction in labor is achieved because we have replaced the many-body heatbath by a single damped oscillator. Thus, in effect, we are modeling the solid by a two atom effective system (see Appendix) which is why our trajectory problem reduces to a three-body calculation. The results derived from these three models will be discussed in section 3.

## 3. Description of the calculation

### 3.1. System studied

For the calculation presented here, we have used parameters appropriate for rare gas/metal systems. For some of the studies, a repulsive potential of the form

$$W(r, R) = D_r \exp[-\alpha_r(Z - z - r_r)], \tag{3.1}$$

is used. The values of $D_r$ and $r_r$ are unimportant as they are merely a shift in the $Z$ axis origin. (They will affect $R_{max}$ in eq. (3.3).) A value of $\alpha_r = 1.8$ Å$^{-1}$ was used. Since the repulsive potential is only going to be used for sample studies, $\alpha_r$ is the same for all masses studied so as to observe the effect of changing the mass. In addition, an attractive Morse potential was used where

$$W(r, R) = D_e\{\exp[-2\alpha(Z - z - r_e)] - 2\exp[-\alpha(Z - z - r_e)]\}. \tag{3.2}$$

The values of the attractive potential parameters are given in table 2.

### 3.2. Selection of initial conditions

To simulate gas–solid scattering one integrates the GLE (2.15) since the potentials given above, eqs. (3.1) and (3.2) are only one dimensional, horizontal momentum will be conserved. Thus only the initial conditions for the equations of motion in the perpendicular or $Z$ direction are given. The initial energy $E_i$ of the gas particle

Table 2
Potential parameters

| System | Parameters | | |
|---|---|---|---|
| | $D_e$ (K) | $\alpha$ (Å$^{-1}$) | $r_e$ (Å) |
| Ne/Ag | 112.0 [a] | 1.8 [b] | 3.01 [b] |
| Ar/Ag | 417.8 [a] | 1.69 [b] | 3.27 [b] |

[a] Ref. [12].
[b] Obtained by the same procedure as given in Lin and Wolken [13], only $\alpha$ is obtained from a fit of the Morse potential to a Lennard-Jones (6, 12) instead of a LJ (3, 9).

is established at the beginning of the calculation. For the gas atom, the initial conditions are

$$Z(0) = R_{max} + \xi P \tau_p / M, \quad P_Z(0) = -P, \tag{3.3}$$

where $\xi$ is a random number between 0 and 1, $P = \sqrt{2ME_i}$, $\tau_p = 2\pi/\omega_0$ is the period of the struck oscillator, and $R_{max}$ is some distance such that

$$\frac{\partial W}{\partial Z}(r, R)|_{Z=R_{max}} \approx 0.$$

The momentum of the gas atom could also be selected from a Maxwell–Boltzmann distribution but that would require Monte Carlo averaging another variable. For the struck solid atom the initial position is the equilibrium position

$$z(0) = 0, \tag{3.4}$$

and the initial momentum is randomly sampled from a Gaussian distribution with the variance equal to $\sqrt{mk_B T_s}$, where the solid temperature is given. The initial positions are allowed to thermalize before the gas atom enters the interaction region; thus they actually have initial values other than 0. The auxiliary variables have an initial value

$$I_\lambda^s(0) = 0, \quad I_\lambda^c(0) = 0. \tag{3.5}$$

As in most classical trajectory techniques several of the initial conditions must be Monte Carlo averaged, in this case they are $p(0)$, and $f(0)$. At $T_s = 0$ K, $p(0) = 0$ and $f(0) = 0$, so that there are no Monte Carlo averages. For an Einstein solid all temperature effects are in the initial momentum of the struck atom, since there is no noise source $f(t)$.

### *3.3. Results and discussion*

We have studied the energy transfer for rare gas/metal systems for each of the models discussed in section 2.5. The initial calculations were done at a solid temperature of $T_s = 0$ K as there are no Monte Carlo averages of the initial solid momentum and of the random force to perform. That is, there is only one trajectory or solution to eqs. (2.15) for a given initial gas energy $E_i$. A repulsive potential eq. (3.1), was used to study the effects of varying the $\Theta_D$, $\alpha_r$, $M$ and $T_s$.

The results from the heatbath Brownian oscillator (hBo) model are obtained by integrating eqs. (2.15) with the gas particle initial conditions as described in section 3.2. The parameters for $\Theta(t)$ in table 1 were obtained by using the Debye density of modes eq. (2.17) to generate a short time $\Theta(t)$ from eq. (2.4) and fitting to the expansion eq. (2.11). The primitive frequency $\omega_0$ is from eq. (2.20). By setting $I_\lambda^s(t) = f(t) = 0$ and then integrating eqs. (2.15a–d), the Einstein model results are obtained. The same primitive frequency $\omega_0$ is used in the Einstein model as the hBo model.

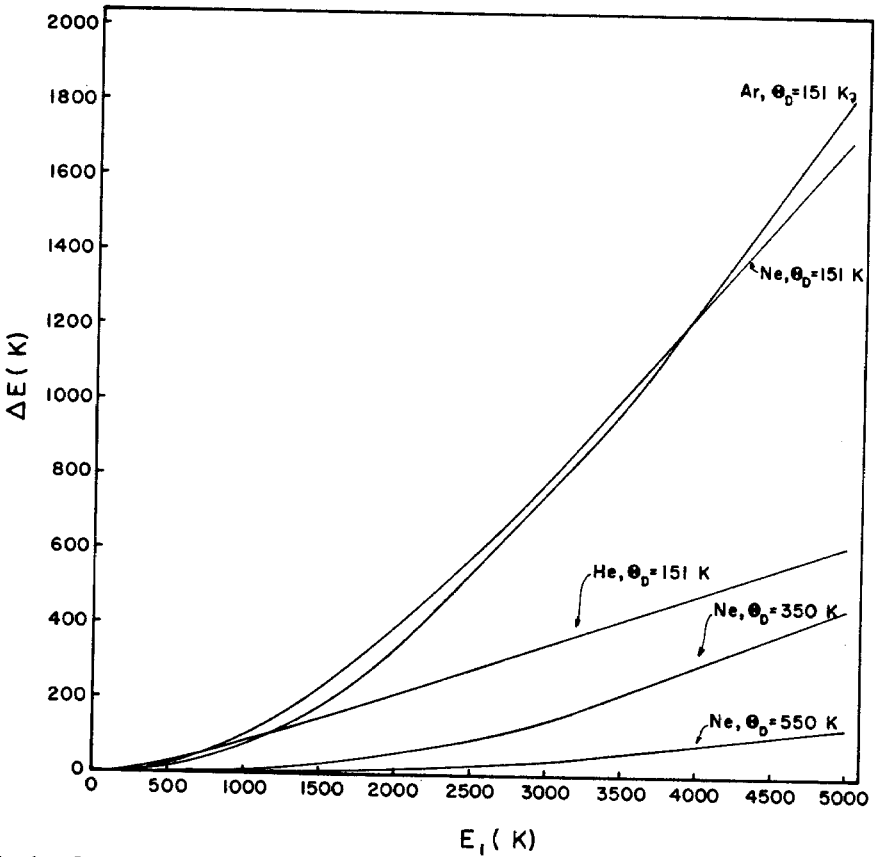


Fig. 1. $\Delta E$ versus $E_i$ for rare gas/Ag scattering. A repulsive interaction potential is used with $\alpha_r = 1.8\ \text{Å}^{-1}$. All curves are for the heatbath Brownian oscillator model.

Finally for the friction model, eq. (2.22a) is substituted for eq. (2.15a) with $\beta$ taken from either eq. (2.14) ($\beta_f$) or eq. (2.21a) ($\beta_D$). Eq. (2.21b) is used for the oscillator frequency $\Omega$.

Fig. 1 displays the energy transfer $\Delta E_{hBo}$ as a function of incident gas energy $E_i$ for He/Ag, Ne/Ag and Ar/Ag scattering using an Ag surface Debye temperature $\Theta_D = 151$ K. Also plotted are $\Delta E$ versus $E_i$ curves for Ng/Ag scattering with $\Theta_D =$ 350 and 550 K. At high energies ($\sim 10^6$ K) the curves approach the hard sphere limit of

$$\Delta E/E_i = 4mM/(m+M)^2 \tag{3.6}$$

From the family of Ne/Ag curves one can see that at constant $E_i$, the energy transfer decreases with increasing $\Theta_D$. A larger $\Theta_D$ corresponds to a stiffer effective spring, thus making it more difficult to transfer energy.

The magnitude of the energy transfer is very sensitive to the parameters $\Theta_D$, $\alpha_r$, $M$, and $T_s$ and to the model, hBo, Einstein or friction, being used. However, ratios of energy transfer (e.g. $R_E = \Delta E_{Einstein}/\Delta E_{hBo}$) should basically depend only on the dimensionless quantity $\omega_D t_c$, where $t_c$ is the collision time. This quantity $\omega_D t_c$ is really a ratio of the collision time to the response time $\tau_D$ of the solid ($\omega_D = 2\pi/\tau_D$), thus $\omega_D t_c$ measures the interaction of the heatbath with the collision process. For a repulsive potential the collision time is naively defined as the range of the potential $1/\alpha_r$ divided by the incident velocity of the gas atom, viz.,

$$t_c = (M/2E_i)^{1/2}/\alpha_r . \tag{3.7}$$

As discussed in section 2.5, the hBo model is qualitatively and quantitatively accurate in describing energy transfer for all collision times. (For really long time processes such as diffusion and desorption this assertion must be tested.) The Einstein model is rigorously accurately in the limit of short collision times but will fail for long times. The friction model is derived as an approximate solution for long collision times but this is not an exact derivation. Thus, plots of $\Delta E_{model}/\Delta E_{hBo}$ should display the time domains in which each model is valid.

The ratio plots for the Einstein model and the friction model using $\beta_f$ and $\beta_D$ are shown in fig. 2. Each frame of fig. 2 actually displays 9 curves. They correspond to $R_E$, $R_f$ and $R_D$ for various values of $\alpha_r$, $\Theta_D$ and $M$. The curves of each family, e.g. $R_E$ are nearly superimposable, with the largest discrepancies appearing when the mass is varied (fig. 2c). As discussed in section 2.5, the Einstein model should be valid for "short" collision times, when the struck oscillator does not have time to feel the heatbath. This is verified in fig. 2, at small $t_c$, $R_E \approx 1$ while for long collision times $R_E \to 0$. Short collision times can only be thought of with respect to the response time of the solid, i.e. $\tau_D$. A smaller $\tau_D$ or larger $\omega_D$ means a greater speed of sound, and thus the lattice responds more quickly to the impinging atom, so that "short" is a relative term. For the friction models on still needs to think in terms of the ratio of $t_c$ to $\tau_D$. Again, the behavior is nearly reproducible for different systems. Neither the results from using $\beta_f$ of eq. (2.14) or $\beta_D$ of eq. (2.21a) are quantitatively accurate for any time regime. In addition, the two $\beta$'s predict different behavior. The friction model is unreliable in describing energy transfer.

Fig. 3 displays $\Delta E$ versus $E_i$ curves for Ne/Ag scattering with the attractive potential of eq. (3.2) for the hBo, Einstein and two friction models at two surface Debye temperatures. The same basic trends appear as in the repulsive potential. The Einstein and friction models are again incorrect. At high collision energies (or short collision times) the hBo and Einstein results approach the hard sphere limit of eq. (3.6). As $\Theta_D$ increases the energy transferred is less and the effect of the heatbath becomes more important. We have also plotted ratio curves in the same manner as fig. 2 for the attractive potential. The basic trends are similar but since the families of curves are not as superimposable, these graphs are not presented here. Although the ratio results are not as superimposable for the attractive potential as for the repulsive potential, it is still $\omega_D t_c$ that is the essential parameter in decribing energy

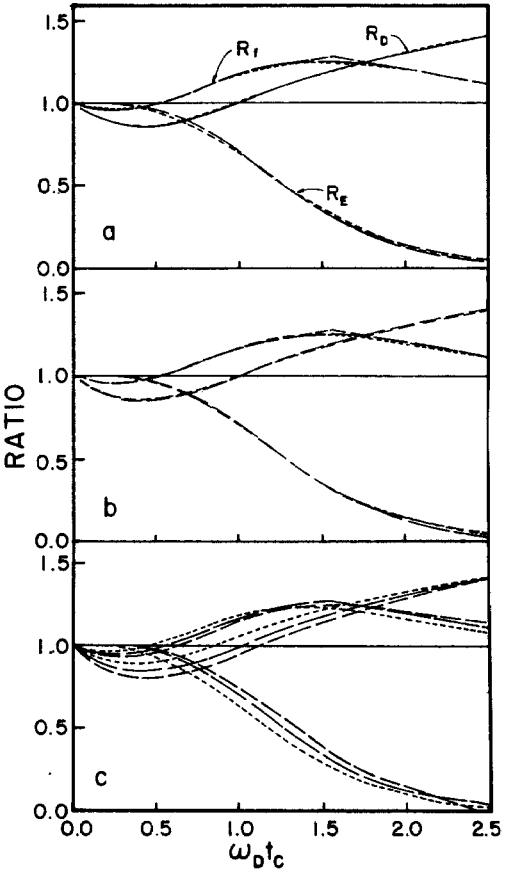


Fig. 2. Ratios of $\Delta E_{\text{model}}/\Delta E_{\text{hBo}}$ as a function of $\omega_D t_c$ (E = Einstein, f = friction model using $\beta_f$, D = friction model using $\beta_D$). The system common to all the graphs is Ne/Ag with $\Theta_D$ = 151 K and $\alpha_r$ = 1.8 $A^{-1}$ (Ne, 151 K, 1.8 $A^{-1}$).
(a) (– – –) Ne, 151 K, 1.0 $A^{-1}$; (— —) Ne, 151 K, 1.8 $A^{-1}$; (- - - - - -) Ne, 151 K, 3.0 $A^{-1}$.
(b) (– – –) Ne, 151 K, 1.8 $A^{-1}$; (— —) Ne, 350 K, 1.8 $A^{-1}$; (- - - - - -) Ne, 550 K, 1.8 $A^{-1}$.
(c) (– – –) He, 151 K, 1.8 $A^{-1}$; (— —) Ne, 151 K, 1.8 $A^{-1}$; (- - - - - -) Ar, 151 K, 1.8 $A^{-1}$.

transfer regimes. Note that at low collision energies, the Ne traps or adsorbs on the surface. This is only important for $\Theta_D$ = 151 K; the trapping thresholds for $\Theta_D$ = 350 K are approximately $E_{\text{trap}} \approx 2$ K.

The behavior of trapping thresholds (the maximum beam energy for which trapping occurs) $E_{\text{trap}}$ as a function of $\Theta_D$ is studied more extensively for the Ar/Ag system at $T_s$ = 0 K. Fig. 4 displays trapping thresholds as a function of $\Theta_D$ for each of the models discussed previously. The Einstein and friction models do not accurately describe the trapping threshold. The energy transfer decreases with increasing $\Theta_D$, thus the trapping threshold must decrease also. Again, as in fig. 3, the influence

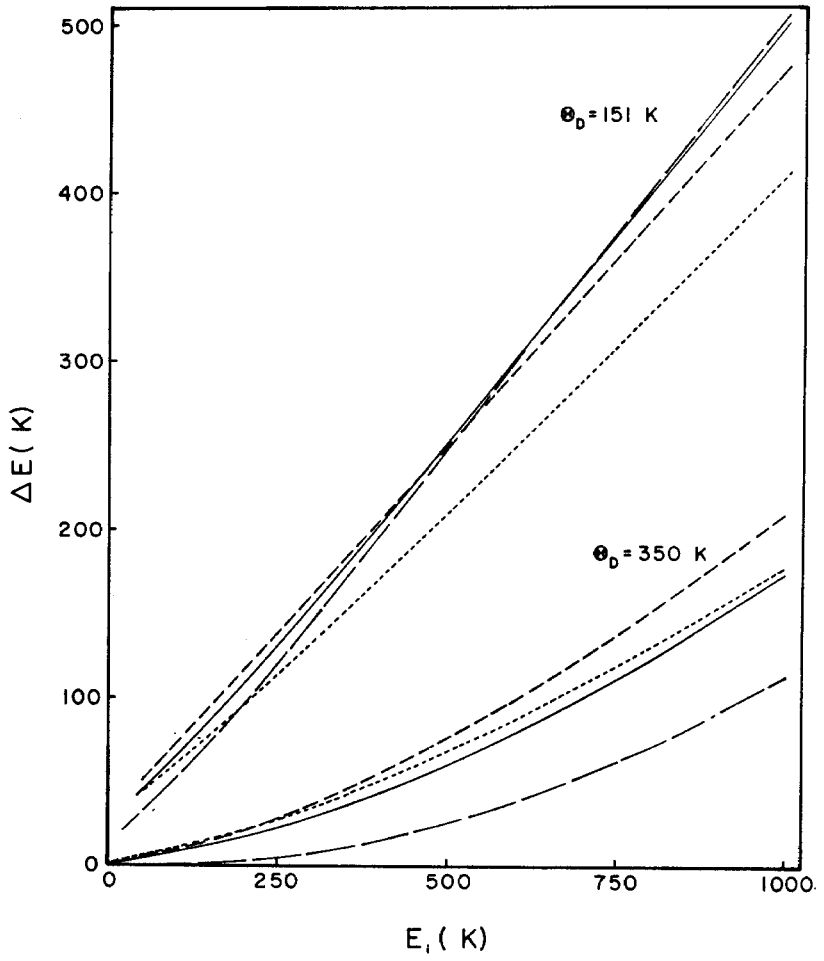


Fig. 3. $\Delta E$ versus $E_i$ for Ne/Ag scattering using an attractive Morse potential: (———) hBo results; (— — —) Einstein model results; (– – –) friction model using $\beta_f$; (- - - - -) friction model using $\beta_D$.

of the heatbath is more important at larger $\Theta_D$, i.e., the ratio of $E_{trap}^{hBo}/E_{trap}^{Einstein}$ increases with $\theta_D$.

So far we have dealt with lattices at $T_s = 0$ K. Our qualitative conclusions about the valid energy regimes of the Einstein and friction models hold for finite lattice temperatures. We illustrate this for Ne/Ag scattering using a repulsive potential, eq. (3.1) with $\alpha_r = 1.8$ Å$^{-1}$ and $\Theta_D = 151$ K. The solid line is the ratio of $\Delta E_{Einstein}/\Delta E_{hBo}$ versus $\omega_D t_c$, reproduced from fig. 2. The discrete points are the various $R_E$ for different incident energies (or collision times) with the solid at $T_s = 100$ K. The error bars arise because at finite solid temperatures the initial momentum of the

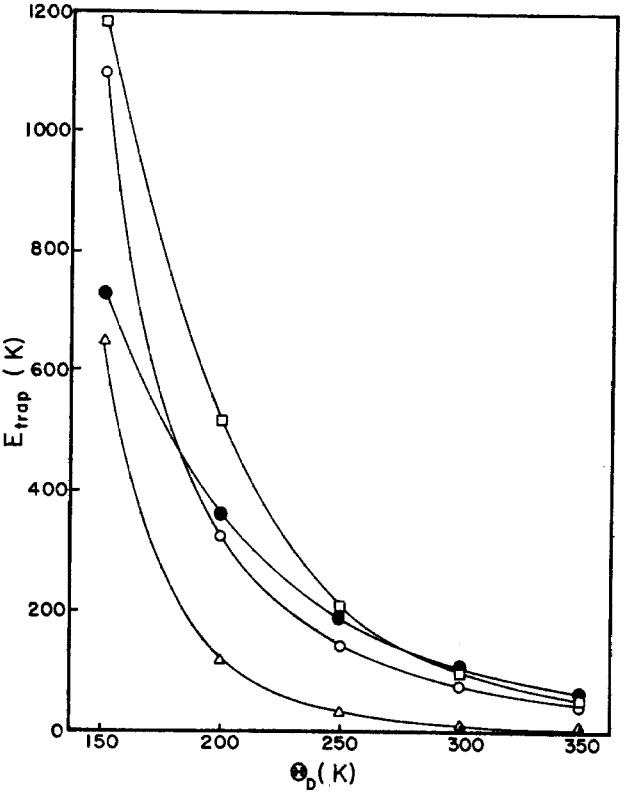


Fig. 4. $E_{trap}$ versus $\Theta_D$ for Ar/Ag scattering: (○) hBo results; (△) Einstein model results; (□) friction model using $\beta_f$; (●) friction model using $\beta_D$.

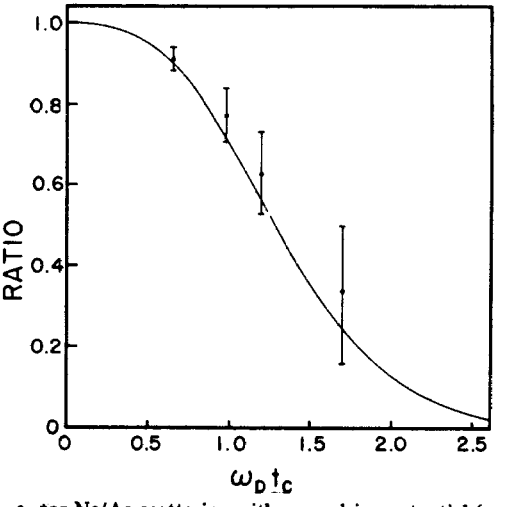


Fig. 5. $R_E$ versus $\omega_D t_c$ for Ne/Ag scattering with a repulsive potential ($\alpha_r$ = 1.8 Å$^{-1}$, $\Theta_D$ = 151 K). The results for $T_s$ = 0 and 100 K are shown by a solid line and discrete points, respectively.

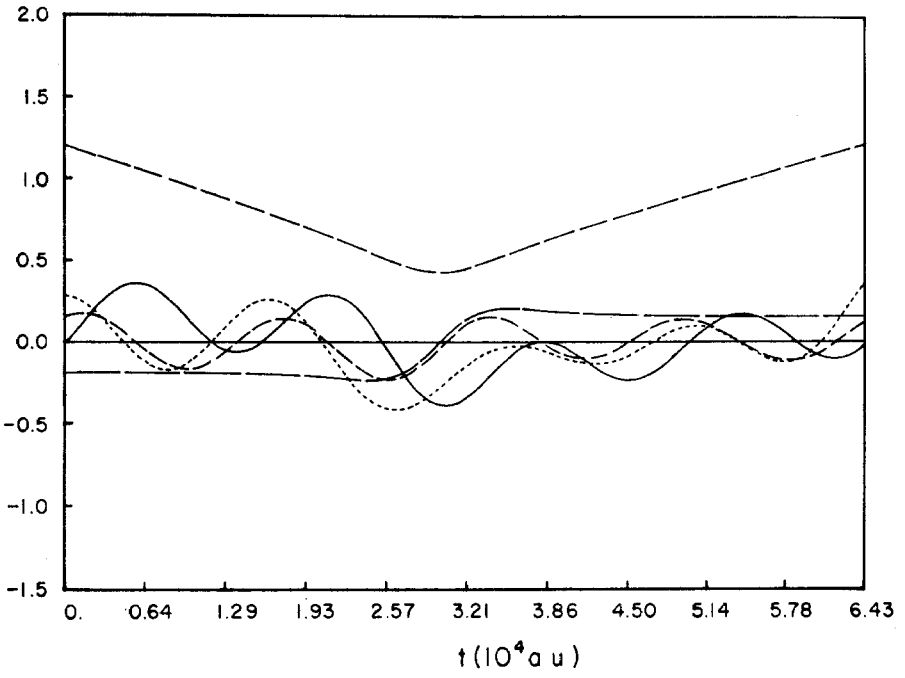


Fig. 6. Sample trajectory of He/Ag scattering at a finite solid temperature, $T_s$ = 296 K. Energy is transferred from the gas to the solid: (---) $Z/10$ (gas); (— —) $P_Z/10$ (gas); (———) $z$ (solid); (------) $P_z/100$ (solid); (· · · · ·) $f \times 100$.

solid and the random force must be Monte Carlo averaged. Typically, around 350 trajectories per $E_i$ per model are required. The qualitative behavior of the curves at $T_s$ = 0 and 100 K is similar; the Einstein model is only valid for short collision times. The magnitudes and direction of the energy transferred between the gas and the solid reflects the amount of energy in the solid, i.e., $T_s$. For the results shown in fig. 5 (for a given $E_i$), $\Delta E(T_s = 100\ \text{K}) < \Delta E(T_s = 0\ \text{K})$.

Figs. 6 and 7 show typical trajectories for gas/solid collisions at non-zero solid temperatures. As can be seen from these figures, the relative motion of the gas and solid particles is critical in deciding whether the gas loses or gains energy. If the solid atom is moving into the solid, the tendency will be to accept energy from the gas (fig. 6). In the opposite extreme where the gas and solid atoms are moving toward each other (fig. 7), it is easier for the gas to gain energy.

## 4. Summary

The generalized Langevin equations (GLE), which are an exact transformation of Newton's equations of motion for a gas particle impinging on an harmonic solid,

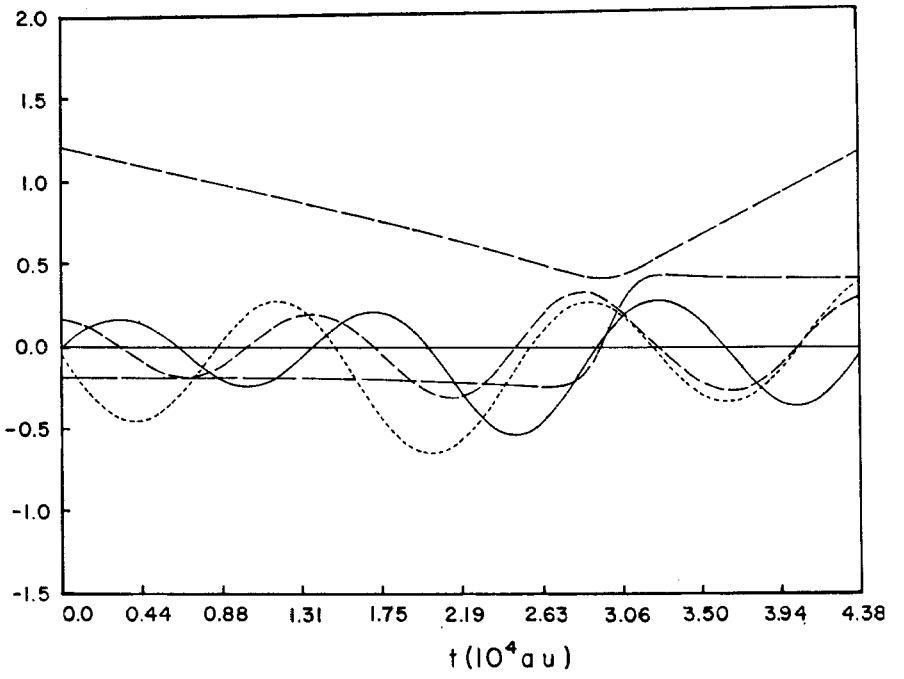


Fig. 7. Same as fig. 6 only energy is transferred to the gas from the solid.

have been recast as coupled first order differential equations soluble by standard classical trajectory techniques. Three physical models are introduced which greatly reduce the dimensionality of the trajectory problem. These are the Einstein and friction models which define effective two-body dynamical problems and the heatbath-Brownian oscillator model which yields a three-body effective trajectory problem. The heatbath-Brownian oscillator model is qualitatively correct for all collision situations.

The GLE have been solved for rare gas/metal scattering using repulsive and attractive potentials. The energy transfer $\Delta E$ of the gas atom obtained from the heatbath-Brownian oscillator model is compared to $\Delta E$'s obtained from Einstein and friction models of the solid. Ratios of theses $\Delta E$'s plotted as functions of the dimensionless quantity $\omega_D t_c$, where $t_c$ is the collision time, show the time domains of validity of the Einstein and friction models. The Einstein model is correct at short collision times but fails at longer times. Here the length of the collision time is with respect to the response time of the solid, $\tau_D = 2\pi/\omega_D$. The friction model does not give the correct behavior at any times.

Trapping thresholds are studied as a function of Debye temperature $\Theta_D$ for Ar/Ag scattering at $T_s = 0$ K. The trapping threshold decreases with increasing $\Theta_D$ and

the effect of the heatbath becomes more important. Again, the Einstein and friction models are incorrect.

## Acknowlegments

We wish to acknowledge partial support of this work by a Research Corporation Cottrell Grant, by the National Science Foundation (MRL program DMR 76-00889) and by the Donors of the Petroleum Research Fund of the American Chemical Society, under Grant S990AC6. Valuable conversations with Dr. Ying-wei Lin are also gratefully acknowledged.

## Appendix

Replacing the true damping function $\Theta(t)$ by a single damped sine function is equivalent to modeling the heatbath by a single Brownian oscillator. More precisely, it is equivalent to replacing the exact gas–solid equations of motion by the following effective three-body equations ($x_h(t)$ is the Brownian oscillator coordinate)

$$M\ddot{R}(t) = -\nabla_R W(r, R), \tag{A.1a}$$

$$m\ddot{r}(t) = -m\omega_0^2 [r(t) - x_h(t)] - \nabla_r W(r, R), \tag{A.1b}$$

$$m\ddot{x}_h(t) = -m\omega_0^2 [x_h(t) - r(t)] - m\omega_h^2 x_h(t) - m\beta_h \dot{x}_h(t) + f_h(t), \tag{A.1c}$$

where the Brownian noise $f_h(t)$ has a white spectrum; i.e.

$$\langle f_h(t) \cdot f_h(0) \rangle = 6mk_B T\beta_h \delta(t), \tag{A.2}$$

Clearly, eqs. (A.1) may be easily solved numerically with $f_h(t)$ chosen from a probability distribution consistent with eq. (A.2). This effective three-particle trajectory problem is completely equivalent to eqs. (2.15) with $N = 1$ and provides an alternative way to reduce the Langevin theory to computationally convenient form.

To establish the connection between eqs. (A.1) and (2.15), we solve eq. (A.1c) for $x_h(t)$ and insert the result in eq. (A. 1b). This gives an equation of the form of eq. (2.1) with $\theta(t)$ given by eq. (2.11) with $N = 1$. This is equivalent to eqs. (2.15) if we choose $\gamma = 1/2\,\beta_h$, $\tilde{\omega}^2 = \omega_0^2 + \omega_h^2 - \frac{1}{4}\beta_h^2$, $C = \tilde{\omega}^{-1}\,\omega_0^4$ in eqs. (2.15).

## References

[1] S.A. Adelman and J.D. Doll, J. Chem. 61 (1974) 4242; 62 (1975) 2518.
[2] J.D. Doll, L.E. Myers and S.A. Adelman, J. Chem. Phys. 63 (1975) 4908.
[3] S.A. Adelman and J.D. Doll, J. Chem. Phys. 64 (1976) 2375.

[4] S.A. Adelman, Chem. Phys. Letters 40 (1976) 495.
[5] For example, M. Karplus, R.N. Porter and R.D. Sharma, J. Chem. Phys. 43 (1965) 3259.
[6] S.A. Adelman and B.J. Garrison, J. Chem. Phys. 65 (1976) 3751.
[7] We employed a fourth order Adams–Moulton predictor corrector integrator.
[8] D.R. Dion and J.D. Doll, J. Chem. Phys. 65 (1976) 3762.
[9] Another procedure for recasting eqs. (2.1) as differential equations has been proposed by M. Shugard, J.C. Tully and A. Nitzan, Dynamics of Gas–Solid Interactions: Model Calculations of Energy Transfer and Sticking (in press).
[10] The problem of calculating $\rho(\omega)$ has been considered by many authors since the work of E. Montroll, J. Chem. Phys. 10 (1942) 218; 11 (1943) 481. For a review of the earlier work see A.A. Maradudin, F.W. Montroll, G.H. Weiss and I.P. Ipatova, Theory of Lattice Dynamics in the Harmonic Approximation, 2nd ed. (Academic, New York, 1971). More recent treatments have been given by J. Deltour, Physica 39 (1968) 413; R.I. Cukier and J.C. Wheeler, J. Chem. Phys. 60 (1974) 4639; O. Platz and R.G. Gordon, Phys. Rev. Letters 20 (1973) 264.
[11] M. Abramowitz and I.A. Stegun, Handbook of Mathematical Functions, (National Bureau of Standards, Washington, DC, 1970).
[12] R. Sau and R.P. Merrill, Surface Sci. 34 (1973) 268.
[13] Y.-W. Lin and G. Wolken, Jr., J. Chem. Phys. 65 (1976) 2634.